Vilidaitė & Baker (2015) *Perception*, 44(5): 541-555
doi: 10.1068/p7819

Unbiased measures of interocular transfer of motion adaptation

Greta Vilidaitė & Daniel H. Baker

Department of Psychology, University of York, Heslington, York, YO10 5DD, UK
email: daniel.baker@york.ac.uk

Abstract

Numerous studies have measured the extent to which motion aftereffects transfer interocularly. However, many have done so using bias-prone methods, and studies rarely compare different types of motion directly. Here, we use a technique designed to reduce bias (Morgan, 2013, *J Vis*, 13(8): 26) to estimate interocular transfer (IOT) for five types of motion: simple translational motion, expansion/contraction, rotation, spiral and complex translational motion. We used both static and dynamic targets with subjects making binary judgements of perceived speed. Overall, the average IOT was 65%, consistent with previous studies (mean over 17 studies of 67% transfer). There was a main effect of motion type, with translational motion producing stronger IOT (mean: 86%) overall than any of the more complex varieties of motion (mean: 51%). This is inconsistent with the notion that IOT should be strongest for motion processed in extrastriate regions that are fully binocular. We conclude that adaptation is a complex phenomenon too poorly understood to make firm inferences about the binocular structure of motion systems.

Keywords: interocular transfer, motion adaptation, bias-free methods.

1 Introduction

Sensory systems adapt to prevailing conditions by dynamically adjusting their sensitivity (Webster, 2011). This canonical process is observed at multiple levels in the visual hierarchy, from retinal adaptation to luminance (Reuter, 2011), through orientation- (Campbell & Maffei, 1971) and spatial frequency-dependent (Blakemore & Campbell, 1969; Blakemore & Sutton, 1969) adaptation in early cortical regions, to more complex dimensions such as curvature (Gheorghiu & Kingdom, 2008), blur (Kompaniez, Sawides, Marcos, & Webster, 2013), numerosity (Liu, Zhang, Zhao, Liu, & Li, 2013), regularity (Ouhnana, Bell, Solomon, & Kingdom, 2013), facial identity (Strobach & Carbon, 2013) or expression (Adams, Gray, Garner, & Graf, 2010), and motion (Mather, Pavan, Campana, & Casco, 2008; Mather, Verstraten & Anstis, 1998).

A key tool in the study of visual adaptation has been measurement of the interocular transfer (IOT) of an aftereffect (e.g. Blake, Overton, & Lema-Stern, 1981). By adapting only one eye, and comparing the strength of the aftereffect measured to target stimuli in the unadapted eye, with that for target stimuli in the adapted eye, the level at which adaptation occurs can be inferred (Moulden, 1980). For example, adaptation to bright light is largely retinal, and so does not transfer between the eyes (Auerbach & Peachey, 1984). On the other hand, adaptation to numerosity presumably occurs at a cortical level beyond the point of binocular combination, and so transfers almost completely (Liu et al., 2013). For contrast adaptation to grating stimuli, transfer of around 60% is typically reported, though this may be reduced at low spatial frequencies (Baker & Meese, 2012).

Motion adaptation is a particularly engaging phenomenon (c.f. the "Waterfall illusion" described by Addams, 1834), and its investigation has a lengthy history (Thompson, 1880). The motion aftereffect (MAE) is the illusory motion induced following adaptation, probed using either static or moving targets (Verstraten, Fredericksen, Van Wezel, Lankheet, & Van de Grind, 1996). Recent converging evidence suggests that motion adaptation may occur at multiple levels in the visual hierarchy (Mather et al., 2008), perhaps involving different populations of neurons depending on whether the test stimuli are static or dynamic. However, the literature on IOT of motion adaptation does not present a particularly clear picture. In part this is because stimuli and

methodologies differ widely between studies (see Table 1 for a summary), and even within studies results can be quite heterogeneous (e.g. Nishida & Ashida, 2000; Tao, Lankheet, van de Grind, & van Wezel, 2003). There is some evidence that more complex motion, such as spiral patterns, might produce stronger IOT than simpler linear motion (Steiner, Blake, & Rose, 1994). This is an appealing notion, as it is consistent with the finding that later visual areas (which are presumably entirely binocular) are responsive to motion from optic flow (Morrone et al., 2000), including spiral motion (Graziano, Andersen, & Snowden, 1994).

Table 1: Summary of 18 studies reporting interocular transfer of motion adaptation. Studies containing several conditions were averaged together first before calculating the mean across studies. Where IOT values were given as a range, we used the midpoint of this range to calculate the mean. Two further studies (Kaunitz, Fracasso, & Melcher, 2011; Maruya, Watanabe, & Watanabe, 2008) were not included as it was not possible to estimate IOT values from the data presented. MOA = method of adjustment.

Reference	**Adapting stimuli**	**Speed of adaptor**	**Type of test stimuli**	**Measure**	**Type of motion**	**IOT (%)**
Holland (1957)	Spiral	50-150 rot/min	Static spiral	Duration	Rotation	70%
Freud (1964)	Spiral	80 rot/min	Static spiral	Duration	Rotation	50%
Mitchell et al. (1975)	Radially striped disc	30 rot/min	Static disc	Manual tracking	Rotation	73%
Wade (1976)	Sectored disc	3.75 rot/min	Static disc	Duration	Rotation	66%
Smith & Over (1979)	Subjective contour gratings	3.68 deg/sec	Static bars	Manual tracking	Linear	58%
Moulden (1980)	Sectored disc	25 rot/min	Static disc	Duration	Rotation	46%
O'Shea & Crassini (1981)	Square-wave gratings	1 deg/sec	Static grating	Manual tracking	Linear	66%
Keck & Price (1982)	Sine-wave gratings	10 deg/sec	Static grating	Duration	Linear	78%
Smith & Hammond (1985)	Square-wave gratings or noise textures	2, 4, 8 deg/sec	2 deg/sec grating/texture	Perceived velocity (MOA)	Linear	45%
Burke & Wenderoth (1993)	Sine-wave plaid	3.55 – 9.7 deg/sec	Static plaid	Duration	Plaid	37%
Raymond (1993)	Random-dot kinematograms	1.83 deg/sec	random-dot kinematogram	Direction discrimination	Linear	96%
Steiner et al. (1994)	Random-dot kinematograms	5.56 deg/sec	random-dot kinematogram	Direction discrimination	Linear Expansion Rotation	76% 91% 86%
Symons et al. (1996)	Random-dot kinematograms	1 deg/sec	Static dots	Duration	Linear	78%
Timney et al. (1996)	Sine-wave grating Spokes Spiral Contracting circles	1 deg/sec 25 rot/min 110 rot/min 2.5 deg/sec	Static grating Static spokes Static spiral Static circles	Duration Duration Duration Duration	Linear Rotation Spiral Contraction	73% 78% 67% 64%
McColl & Mitchell (1998)	Square-wave gratings Random-dot kinematograms Spiral	1.83 deg/sec 1.84 deg/sec Not given	Static grating Random dot kinematogram Static spiral	Perceived velocity Direction discrimination Duration	Linear Linear Spiral	72% 99% 58%
Nishida & Ashida (2000)	Sine-wave gratings	5 deg/sec	Static grating Counterphasing grating	Direction discrimination Duration	Linear Linear	66% 102%
Tao et al. (2003)	Noise texture	0.75-24 deg/sec	Noise texture	Direction discrimination	Linear	58%
					Mean	**67%**

A potential problem with this literature is that previous studies have used measurement techniques that may be subject to substantial biases (Morgan, 2013). For example, one of the most widely-used techniques for measuring the motion aftereffect is to present a static test stimulus following adaptation, and ask the observer to indicate when it appears to stop moving. Because human reaction times cannot be infinitely fast, it is impossible to record the absence of an aftereffect using this technique, and such a subjective method is open to influence from a range of biases and criterion effects. In general, these might be expected to increase the estimates of IOT, as observers might tend to overestimate the strength of a weak dichoptic aftereffect.

Recently, Morgan (2013) has described a technique for measuring adaptation effects that avoids these biases. The technique involves adapting two locations simultaneously in opposite directions. Test stimuli then appear in both locations, moving in one of a variety of direction combinations relative to their adaptors. The observer indicates which of the two test stimuli appears to be moving faster. This avoids the use of simple heuristics and priors associated with paradigms in which only one region is adapted (such as 'things in the adapted region tend to move faster') that can lead to biased responding. Indeed, the paradigm is sufficiently complex (see *Procedures*) that even a highly experienced observer would find it almost impossible to perform in a deliberately biased manner (see Morgan, Dillenburger, Raphael, & Solomon, 2012).

We implemented this paradigm to investigate IOT of the MAE. To address the hypothesis that IOT is stronger for more complex types of motion, we used a variety of motion types, including translational motion, expansion/contraction, rotation, and spiral motion. In addition, we measured IOT for both a dynamic and a static target stimulus. Our aim was to provide a clear and complete picture of IOT using a single paradigm and consistent set of multi-element stimuli, with the same observers completing all conditions.

2 Methods

Apparatus and stimuli

All stimuli were displayed on an Iiyama VisionMaster Pro 510 CRT monitor. The monitor was gamma corrected, had a mean luminance of 40 cd/m^2, a resolution of 1152x870 pixels, and was driven at a refresh rate of 75Hz. Stimuli were created in Matlab, and displayed using Psychtoolbox 3 (Brainard, 1997; Pelli, 1997) using an Apple Macintosh computer. The display was viewed through a mirror stereoscope, to enable separate stimulation of the left and right eyes by displaying images on either side of the screen. The optical viewing distance was 65cm, which yielded a pixel density of 32*pix/deg*. A chin and head rest ensured that observers were positioned correctly.

Stimuli were discs (radius 3.25 degrees) comprised of multiple Gabor micropattern elements (Amano, Edwards, Badcock, & Nishida, 2009a), the orientation and drift rate of which could be set individually. The simplest arrangement was when the elements all had the same orientation, and drifted either upwards or downwards at the same speed (linear motion, see Figure 1a). Radially angled elements produced rotational motion (Figure 1c), and concentric elements produced expanding or contracting motion (Figure 1d), when their speed was proportional to their distance from the centre of the array (e.g. Snowden & Milne, 1997). This was defined as $s_i = r_i * s_{max}$, where s is the speed of each element (i), r is the radius of the element relative to the edge of the disc (scaled 0-1), and s_{max} is the maximum speed of the array. We also produced spiral motion by combining these two manipulations (Figure 1e). Finally, we created stimuli for which the global motion vector was either upwards or downwards, but the local elements had random orientations (distributed uniformly in the range ±60° from horizontal). For these stimuli (which we term complex translational motion, see Figure 1b), the drift rate of each element was proportional to the sine of the angle between the element orientation and the global orientation (see Amano et al., 2009a).

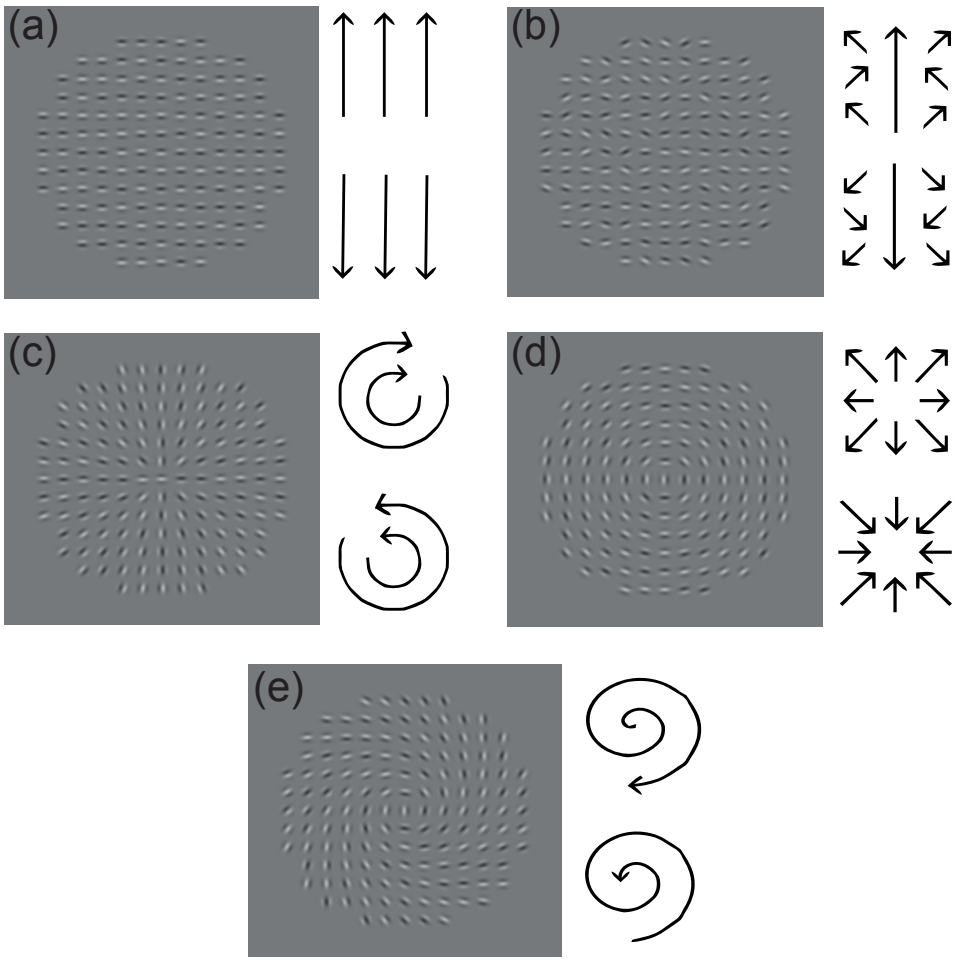

Figure 1. Examples of stimuli with icons depicting motion direction: (a) linear motion upward/downward; (b) complex translational motion with random local orientations and upward or downward global direction; (c) rotational motion; (d) expansion/contraction; (e) spiral motion.

All Gabor elements had a spatial frequency of 4*c*/*deg*, and a full-width-at-half-height of 0.83 carrier cycles, and were displayed at 50% Michelson contrast with random spatial phase. Adapting stimuli for linear motion drifted beneath their Gaussian envelopes (the position of which did not change) at a constant speed of 1.5*deg*/*sec*. For the other types of motion, the most rapidly drifting element in the pattern (those furthest from the centre for rotation, expansion and spiral motion) also drifted at 1.5*deg*/*sec*, and all other elements drifted proportionally slower, as outlined above. The test stimuli on each trial had a range of speeds , determined either by a staircase (Experiment I) or the Method of Constant Stimuli (Experiment II) and were moving either in the same directions as the adapter stimuli or in the opposite directions. They were of the same spatial layout, frequency and element orientation as the adapter stimuli. The elements in the complex translational motion test stimuli had orientations in the range of ±60° from horizontal in the same way as complex translational motion adapter stimuli.

Procedures

To avoid issues of bias, we extended the method outlined by Morgan (2013) to measure interocular transfer. Two adaptors were placed on either side of fixation (offset by ±4.5 degrees), moving in opposite directions (upwards or downwards). Observers were adapted for 120 seconds at the start of each block, and for 5 seconds in between each trial. The absolute direction of the adaptors was counterbalanced across blocks, with observers adapting to only one type of motion and absolute adaptor direction on a given day. In order to reduce local adaptation effects, the orientations of the complex translational motion stimulus (see above) were resampled every 5 seconds during initial adaptation, and for each trial and top-up adaptation period. This was not possible for the other types of

motion, for which motion direction covaried with orientation.

We ran two experiments, to estimate interocular transfer for both the dynamic (Experiment I) and static (Experiment II) motion aftereffect. In both experiments, we used a two-alternative speed matching paradigm, in which observers judged which of two stimuli (presented for 500ms) appeared to be moving fastest. One of these stimuli was the target, which drifted with a maximum speed of 1*deg/sec* (Experiment I) or was static (Experiment II). The other stimulus was the match, the speed of which was determined either by a one-down-one-up staircase (Experiment I; see Meese, 1995), which terminated after 12 reversals, or the Method of Constant stimuli (Experiment II). We used different methods in the two experiments because the unusual psychometric functions (see Figure 7b) that we anticipated finding in the static condition would have interfered with the staircase procedure.

In Experiment I, there were four types of trial, determined by the drift direction of the target and match stimuli relative to the drift direction of the adaptors. When the target and match drifted in the same direction as their respective adaptors (see Figure 2a) we would expect that any effects of adaptation apply equally to both stimuli, and so should not affect the point of subjective equality (PSE) for the match speed. The same veridical perceived speed would be expected when the target and match both drift in the opposite direction to their respective adaptors (Figure 2b). Both of these arrangements constitute control conditions (see Morgan, 2013), and are included in the design with the aim of reducing response bias. The other two conditions are expected to show the effects of adaptation. When the variable-speed match moves in the opposite direction to its adaptor, and the fixed-speed target moves in the same direction as its adaptor, we expect that the perceived speed of the match will increase and the perceived speed of the target will decrease (Figure 2c). This means that the match will need a lower physical speed to appear to move at the same speed as the target, and so the PSE will shift to the left (see example in Figure 4a). When the variable-speed match moves in the same direction as its adaptor, and the fixed-speed target moves in the opposite direction to its adaptor, we expect that the perceived speed of the match will decrease and the perceived speed of the target will increase (Figure 2d). This means that the match will need a higher physical speed to appear to move at the same speed as the target, and so the PSE will shift to the right (see example in Figure 4b).

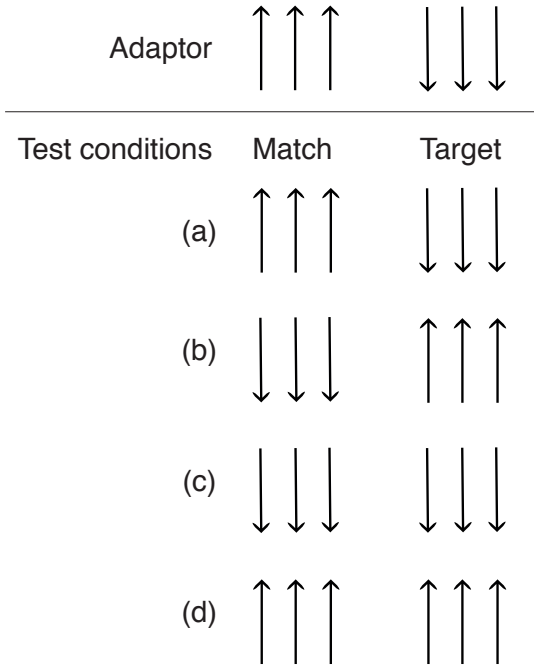

Figure 2: Illustration of different match and target motion directions, relative to the motion of their co-located adaptor (top row). The conditions in which the match and target move in opposite directions (a,b) are control conditions in which adaptation is expected to have no net effect. The conditions in which the match and target move in the same direction (c,d) should produce differential adaptation effects that result in shifts of the PSE for perceived speed. Relative directions are illustrated for linear motion, but the same principle applied for the other varieties of motion.

Trials from the four conditions were randomly interleaved throughout a block. In addition, in half of the trials the target and match stimuli were shown to the same eye as their co-located adaptor to measure monocular adaptation. In the remaining trials, the target and match were shown to the other eye from their adaptors, to measure dichoptic adaptation (as explained in Figure 3). Assignment of match and target to the left and right of fixation was randomly determined on each trial. This deliberately complex design (see Morgan, 2013) ensured that observers were not able to respond in a biased way, as might occur with more traditional paradigms (e.g. by always reporting that stimuli in an adapted location appeared faster). In Experiment I observers completed an average of 79 trials per condition. In Experiment II observers completed 160 MCS trials per condition.

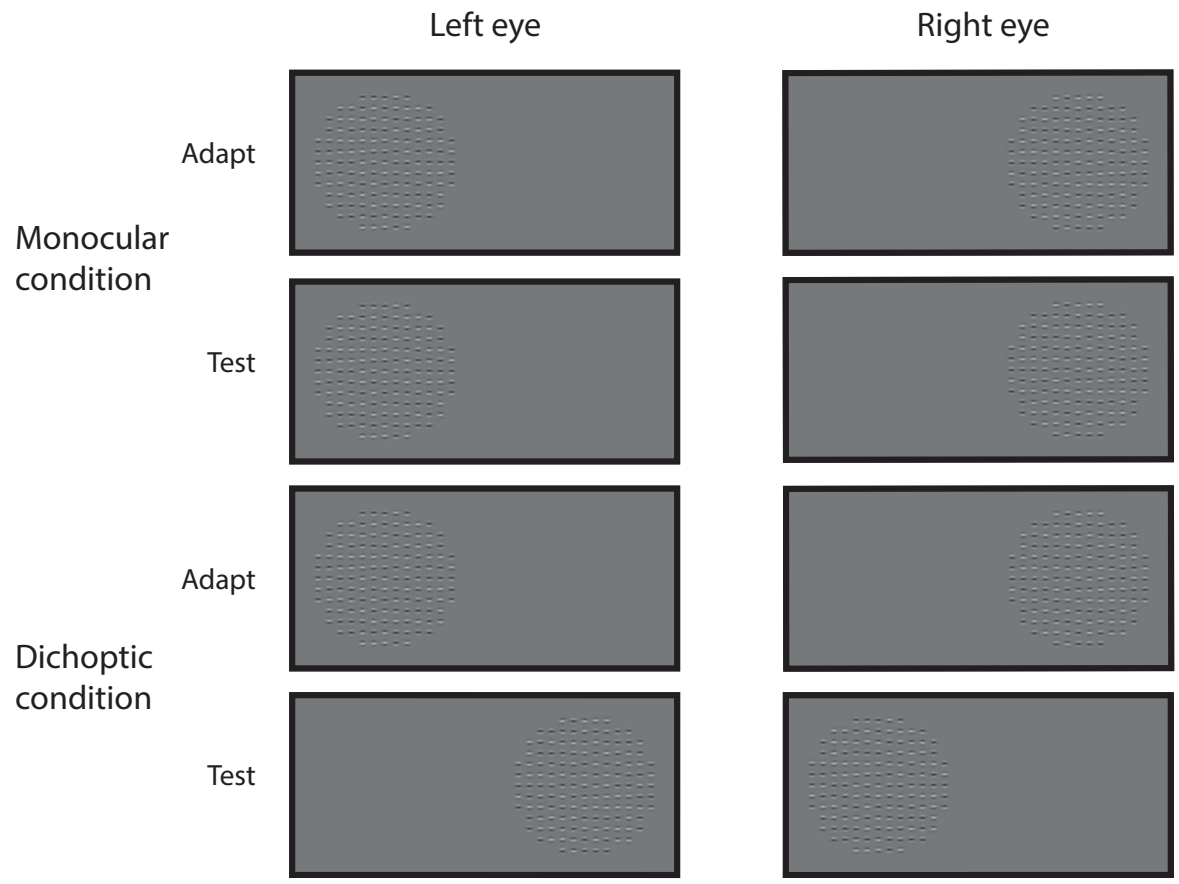

Figure 3. Illustration of the monocular and dichoptic condition designs. In the monocular condition (upper two rows) the test stimulus was presented to the same eye as the adaptor stimulus. In the dichoptic condition (lower two rows) if the adapter was presented on one side of the display to one eye then the test would appear on the same side of the display but to the opposite eye.

Participants

The experiment was completed by both authors, and two naïve observers who were not aware of the purpose of the experiments. Observers gave informed consent, and all procedures were approved by the local ethics committee and were consistent with the original Declaration of Helsinki. All observers completed practice sessions to ensure that they were familiar with the task. During testing, observers wore their normal optical correction if required.

3 Results

Experiment I - dynamic motion aftereffects

When the target was dynamic, we fitted cumulative Gaussian functions to the data to estimate the point of subjective equality (PSE) at 50% 'faster' judgements. Example psychometric functions are shown in Figure 4a,b. In Figure 4a, the target stimulus moved in the same direction as its co-located adaptor, and the match stimulus moved in the opposite direction to its co-located adaptor. This meant that the adaptation effects also worked in opposite directions, reducing the perceived target speed, and increasing the perceived match speed. The PSE (given by the dashed vertical lines in Fig 3a) therefore shifted to slower speeds (a leftward shift of the psychometric function), as slow physical speeds were required for the match to equal the target in perceived speed. The reverse situation is apparent in Figure 4b, where the target stimulus moved in the opposite direction to its adaptor. This shifted the PSE (dashed lines) towards faster speeds.

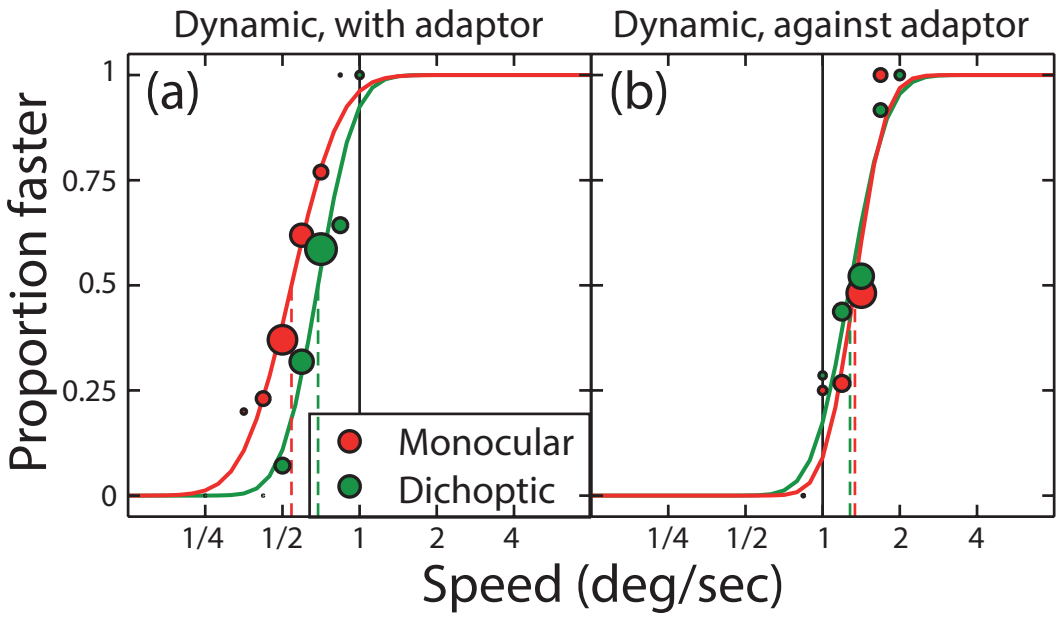

Figure 4: Example psychometric functions for dynamic targets. Values on the ordinate indicate the proportion of trials on which the match stimulus was judged to be moving faster than that target. Symbol size is proportional to the number of trials at each speed. Curves are the fits of cumulative Gaussian functions. Dashed lines indicate the PSE inferred from the curve fits. The black vertical line in each panel gives the true speed of the target.

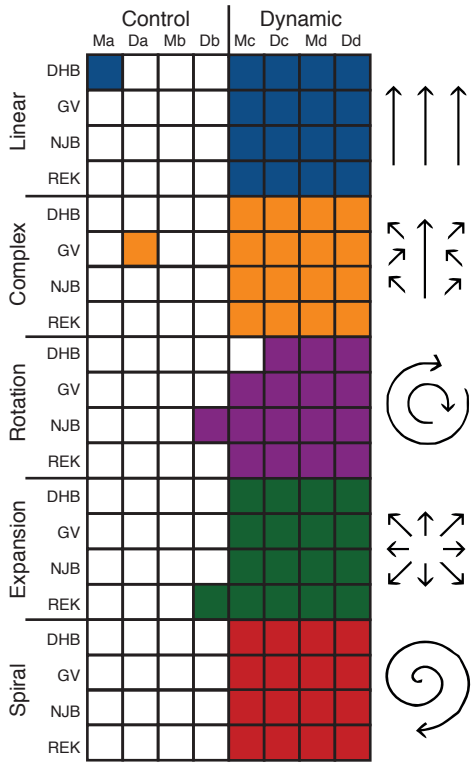

Figure 5: Summary of bootstrapped statistics. Coloured cells indicate conditions in which the bootstrapped 95% confidence limits of the PSE did not overlap the true target speed of 1*deg/sec*. These are conditions in which adaptation had an effect. Column headings: M=monocular, D=dichoptic, the lower case labels (a-d) refer to the adaptor-relative motion conditions detailed in Figure 2. The different rows for each motion type correspond to different observers (DHB, GV, NJB and REK).

We also included control conditions where the match and target both moved in the same or opposite direction to their adaptors. In these conditions the adaptation effects were expected to cancel, and PSEs should match the physical target speed (not shown). We performed bootstrap resampling on each psychometric function, to calculate a population of 1000 simulated thresholds. When the true target speed (1 *deg/sec*) lay outside the 95% confidence limits of this population we considered that adaptation had affected perceived speed. Figure 5 summarises the results of this test for Experiment I, for the control conditions (leftmost four columns) and the conditions in which we expect adaptation to have a measurable effect (rightmost four columns). Significant adaptation effects (coloured cells) were observed for 79/80 psychometric functions in the main conditions but only 4/80 of the control conditions. This equals the expected false positive rate of α=0.05, so we can conclude that the control conditions were not affected by adaptation. This also confirms that our methods were successful in avoiding bias.

Figure 6a shows the monocular PSEs for the case where the target motion was in the same direction as the adaptor. We observed a robust adaptation effect for all motion types, with PSEs shifting by a factor of 1.6-3. The weakest adaptation effect was for complex translational motion (see *Apparatus and stimuli*), and the strongest was for expansion. The finding that more complex forms of motion produce larger MAEs has previously been reported

by Bex, Metha and Makous (1999). A similar but inverted pattern was observed when the target motion was in the opposite direction to the adaptor (Figure 6b). However here the overall effects were weaker (PSE shifts of around a factor of 1.4).

We calculated interocular transfer by dividing the dichoptic PSE shifts by the monocular PSE shifts for each condition (Bjorklund & Magnussen, 1981). The lower panels of Figure 5 show these values expressed as a percentage for each motion type. We observed stronger IOT (around 100%) in the linear and complex translation conditions (blue and orange bars) than in the rotation, expansion and spiral conditions (around 50%; purple, green and red bars). These differences were consistent across the two directions of PSE shift from Figure 6a,b.

A 2x5 repeated measures ANOVA performed on the IOT values revealed a significant effect of motion type ($F_{4,12}$=28.70, p<0.001, partial η^2=0.91). Planned contrasts revealed that all motion types differed from the linear motion condition (all p<0.05). Despite a trend for stronger IOT in the condition where the target speed increased (mean of 79% vs 63%), there was no significant effect of target direction ($F_{1,3}$=9.32, p=0.055). There was also no interaction between target direction and motion type ($F_{4,12}$=0.56, p=0.694).

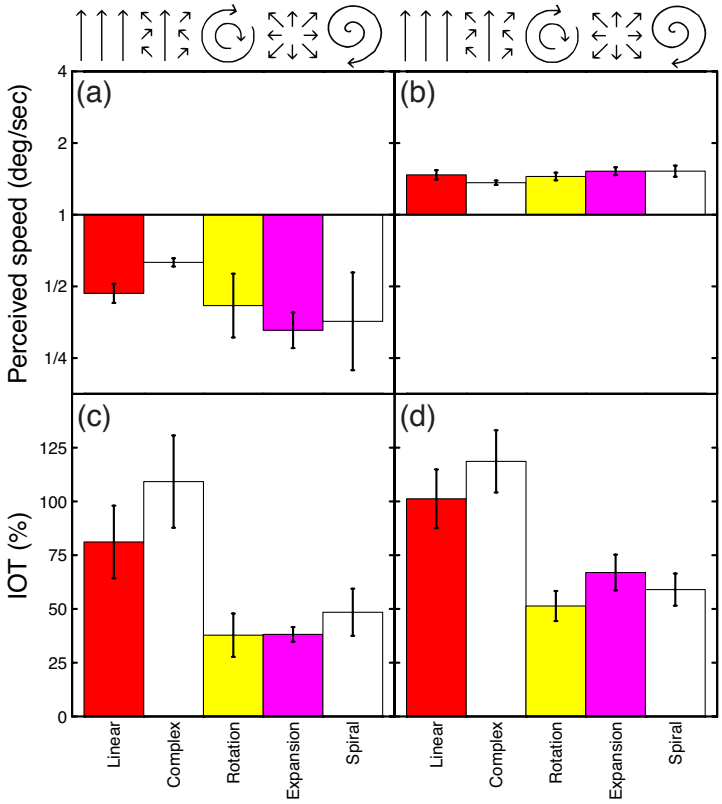

Figure 6. Mean monocular perceived speeds and IOT values across participants for the dynamic MAE. (a) PSE values when the match moved in the opposite direction to its adaptor and the target moved in the same direction as its adaptor (see Figure 2c and Figure 4a); (b) PSE values when the match moved in the same direction as its adaptor and the target moved in the opposite direction to its adaptor (see Figure 2d and Figure 4b); (c,d) mean interocular transfer for each of the conditions in (a,b). Error bars give ±1SEM.

Experiment II - static motion aftereffects

The static MAEs were obtained by using the Method of Constant Stimuli. The target stimulus was always static whereas the matching stimulus moved in either the same or opposite direction to the adaptor. When the matching stimulus moved in the opposite direction to its adaptor, the physical match speed summed with the illusory speed (we refer to this as the 'speeds add' condition). Perceptually, both the static target stimulus and the moving match stimulus appeared to move and their speeds could be estimated as easily as when both had physical motion (e.g. in Experiment I) from the 500ms presentation. This meant that the task became one of speed discrimination, and the psychometric function would be expected to run from 50% correct to 100% correct. We therefore defined threshold for this 'speeds add' condition to be 75% 'match faster' responses (see Figure 7a).

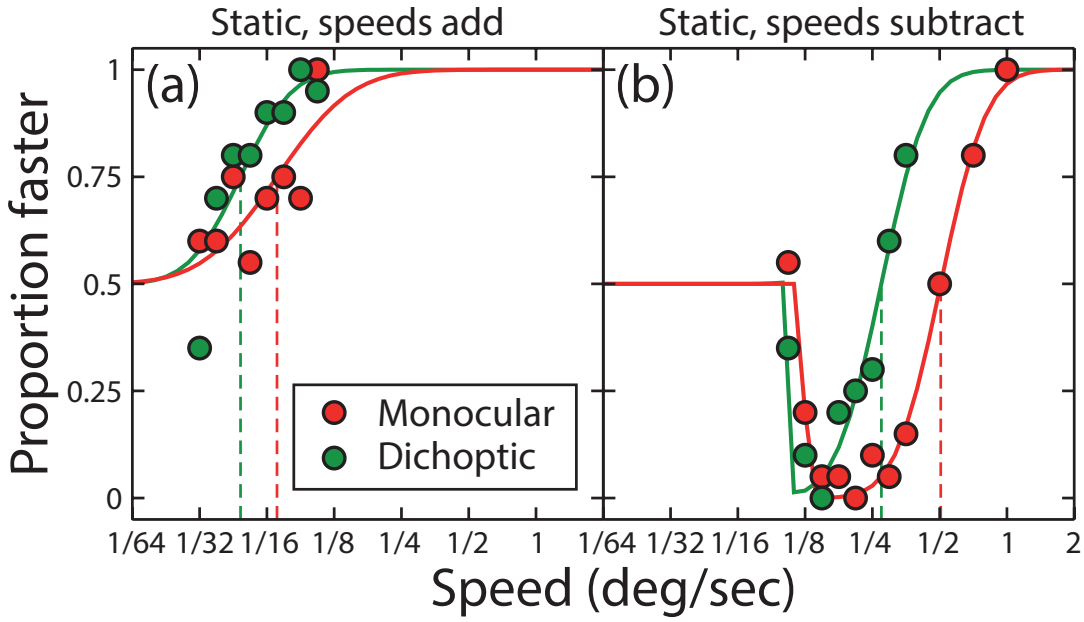

Figure 7: Example psychometric functions for Experiment II. In panel (a) the physical match speed summed with the illusory speed induced by the adaptor, and observers performed a speed discrimination task. In panel (b) the physical motion was opposite in direction to the illusory motion, so first had a nulling effect that caused 'faster' judgements to drop below 50%. At faster speeds the physical motion exceeded the illusory motion but in the opposite direction, increasing the proportion of 'faster' judgements towards 1.

When the matching stimulus moved in the same direction as its adaptor, slow physical match speeds would be expected to cancel (null) the illusory motion. This means that over a range of speeds, the match would be less likely to be judged as faster than the target. But for speeds beyond this, the match would overcome the illusory motion and eventually be judged as faster than the target. These effects would be expected to produce an unusually shaped psychometric function, that drops below 50% faster, and then climbs up to 100% faster (see Figure 7b for examples). (Note that although the functions superficially resemble those reported previously (Baker, Meese, & Georgeson, 2013; Serrano-Pedraza & Derrington, 2010), this is entirely coincidental.) We therefore fitted the data with a pair of cumulative Gaussians, the first of which was constrained to have negative slope and run from 0-0.5, and the second to have positive slope and run from 0-1. We took as our dependent variable the point at which the rising portion of the function intersected 50% faster. This is the point at which the perceived speed of the match equalled that of the target, but in the direction opposite to its own illusory motion (we refer to this as the 'speeds subtract' condition).

Observers required very little physical motion to perform the speed discrimination task in the 'speeds add' case, with discrimination thresholds in the monocular adaptation typically below 0.125*deg/sec* (Figure 8a). Monocular PSE values in the 'speeds subtract' case typically exceeded 0.25*deg/sec* (Figure 8b). As shown in Figure 8c,d, the strongest static IOT was observed in the linear motion condition (>70%), with average IOT values in the other conditions being weaker (typically <60%).

We performed a 2x5 repeated measures ANOVA on the IOT values for the static MAE. The mean IOT for speed discrimination (speeds add, 67%) was significantly greater than that for nulling (speeds subtract, 50%), ($F_{1,3}$=17.60, p<0.05, partial η^2=0.85). As observed with the dynamic MAE in Experiment I, there was a significant effect of motion type ($F_{4,12}$=9.69, p<0.001, partial η^2=0.76), with linear motion differing from all other motion types (all p<0.05) except for spiral motion (p=0.059) in planned contrasts. There was no interaction between the two variables ($F_{4,12}$=1.86, p=0.182).

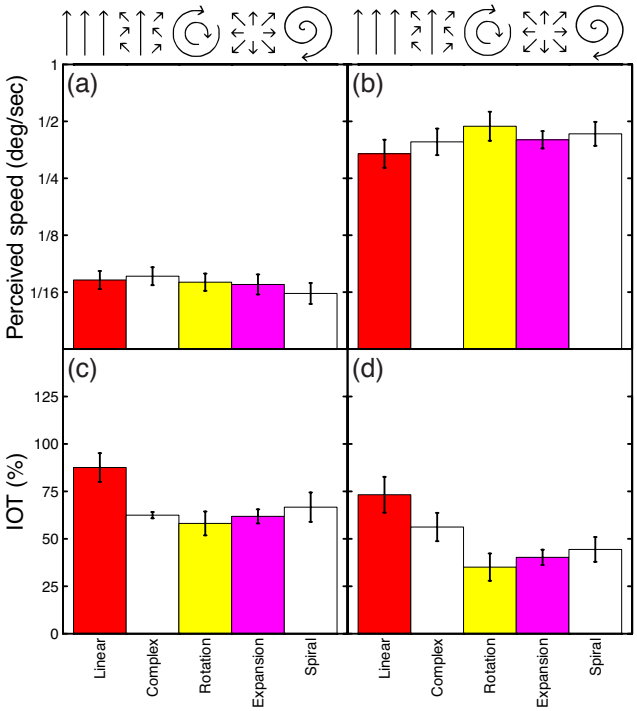

Figure 8. Mean monocular perceived speeds and IOT values across participants for the static MAE. (a) Speed discrimination thresholds when the physical match speed sums with the illusory motion (see Figure 7a); (b) PSE values when the perceived match speed equalled the speed of illusory motion for a static target, but in the opposite direction (see Figure 7b); (c,d) mean interocular transfer for each of the conditions in (a,b). Error bars give ±1SEM.

4 Discussion

We measured interocular transfer of the motion aftereffect using a method designed to minimise bias. The average IOT across all conditions was 65%, consistent with the mean across previous studies of 67% (see Table 1). As far as we are aware, this is the first study that has used the same stimuli to directly compare IOT for both dynamic and static MAEs and also measure IOT for a range of different motion types (linear, complex, rotation, expansion and spiral). There was clear variation in IOT between static and dynamic measures and across different motion types. The dynamic MAE typically produced stronger IOT than the static MAE, consistent with the notion (Mather et al., 2008) that dynamic measures probe later stages of processing (beyond V1).

Architectures for cortical motion processing

Previous studies have suggested that elaborate forms of motion (e.g. rotation, expansion, spiral) might produce stronger IOT than simple linear motion (Steiner et al., 1994). The logic behind this is that the units that integrate more sophisticated motion exist in extra-striate areas (such as MT and MST) that are largely binocular, whereas linear motion might also be encoded by monocular neurons in V1. However, surprisingly few studies have directly compared relevant conditions (see Table 1), and not all those that have found evidence supporting this arrangement (McColl & Mitchell, 1998; Timney et al., 1996). Our experiments find the opposite pattern of results, with translational motion typically producing stronger IOT (mean of 86%) than motion requiring large receptive fields (mean of 51%) (see Figure 6c,d and Figure 8a,b).

Within the traditional framework for understanding interocular transfer these findings would suggest, somewhat counterintuitively, that simple linear motion is processed at a later, more binocular, stage than more elaborate motion. This seems unlikely, given the wealth of studies that have found selectivity for complex motion in later visual areas using fMRI (Morrone et al., 2000), single cell recording (Graziano et al., 1994), EEG (Kremláček, Kuba, Kubová, & Chlubnová, 2004) and MEG (Holliday & Meese, 2008).

An alternative explanation is that early monocular units responding to the linear motion of each of the elements comprising the adapting pattern may have a larger impact on mechanisms that pool over many such units (to compute expansion, contraction or spiral motion) than those which pool over few units (to compute linear motion). A consequence of this might be that the stimuli used in our experiments promote adaptation at early stages, leading to

weaker IOT. Previous studies have developed techniques to separately probe adaptation at different levels of processing (Amano et al., 2012; Lee & Lu, 2014; Lee & Lu, 2012; Scarfe & Johnston, 2011), which might shed light on this issue in future work. Nonlinearities in pooling at different stages and in different areas might further influence the adaptation process, perhaps differentially in cortical regions with varying receptive field sizes (Amano, Wandell, & Dumoulin, 2009b). The adaptation paradigm could be readily adapted to fMRI to test the sensitivity of relevant brain regions, and a detailed computational model might aid understanding of the present psychophysical findings.

Adapting to complex translational motion

We also ran a novel 'complex' translational motion condition, in which the global pattern motion could not be determined from an individual element (Amano et al., 2009a). This produced mixed results, with very strong IOT (around 100%) for dynamic targets (Figure 6c,d) but relatively weak IOT (50-60%) for static targets (Figure 8a,b). This difference was more dramatic than that observed between static and dynamic measures for the other motion types. This is consistent with suggestions that static and dynamic aftereffects arise at different stages of processing (Verstraten et al., 1996), with differential levels of IOT in the direction observed here (discussed in Mather et al., 2008).

In the complex translation condition, the orientations (and therefore speeds) of the individual elements were resampled every 5 seconds during adaptation to avoid adapting spatially local mechanisms. In the dynamic case, this might explain the essentially complete IOT we observed, as any local orientation-tuned detector in monocular areas of cortex stimulated by the target (or match) will have a low probability of having been strongly adapted. We also note that this condition produced the weakest monocular dynamic MAE (orange bars in Figure 6a,b), perhaps indicating that adaptation was occurring at fewer stages than for the other motion types. Thus, it seems that the complex translational motion condition most closely conforms to the predictions about binocularity and IOT.

What is the best measure of adaptation?

Aside from issues of bias, there is one clear difference between our studies and those summarised in Table 1. The present study used an estimate of perceived speed (Thompson, 1981), whereas the majority of previous studies measured the duration of the aftereffect. Changes in perceived speed are a rapid measure, that index the adaptation effect near its peak, whereas duration estimates index the decay of the effect. The only other study to measure IOT using perceived speed (Smith & Hammond, 1985) also found that linear motion from an adaptor with a single orientation produced more IOT than complex motion (from broadband noise textures). This raises the possibility that the aftereffects that are being measured by these two different dependent variables could be distinct, and may not necessarily be highly correlated.

At the suggestion of a reviewer, we tested two experienced participants on a duration version of the experiment. Adaptors were presented for periods of 60 seconds in the same configuration as in the main experiments. A static test stimulus was then presented in both adaptor locations until the participant pressed a button to indicate that illusory motion had ceased. We repeated this procedure for ten trials each of monocular and dichoptic target presentation. The pattern of IOT across the five motion types closely mirrored that from our main experiments, being stronger for linear (mean 79%) and complex (mean 75%) translational motion than for rotation (mean 58%), expansion/contraction (mean 51%) and spiral (mean 58%) motion types. Although this suggests that psychophysically experienced observers are relatively immune to the potential issues of bias outlined in the Introduction, we agree with Morgan (2013) that bias-free methods should be used where possible.

Summary

In summary, our data are not consistent with the idea that the hierarchy of motion adaptation stages can be probed meaningfully by measuring interocular transfer. However, we provide estimates of IOT for a range of motion types, using a consistent method designed to avoid issues of bias. We conclude that adaptation is a complex phenomenon too poorly understood to make firm inferences about the binocular structure of motion systems.

5 References

Adams, W. J., Gray, K. L. H., Garner, M., & Graf, E. W. (2010). High-level face adaptation without awareness. *Psychol Sci*, *21*(2), 205–10. http://doi.org/10.1177/0956797609359508

Addams, R. (1834). An account of a peculiar optical phenomenon seen after having looked at a moving body. *London and Edinburgh Philosophical Magazine and Journal of Science*, *5*, 373–374.

Amano, K., Edwards, M., Badcock, D. R., & Nishida, S. (2009). Adaptive pooling of visual motion signals by the human visual system revealed with a novel multi-element stimulus. *J Vis*, *9*(3), 4.1–25. http://doi.org/10.1167/9.3.4

Amano, K., Takeda, T., Haji, T., Terao, M., Maruya, K., Matsumoto, K., … Nishida, S. (2012). Human neural responses involved in spatial pooling of locally ambiguous motion signals. *Journal of Neurophysiology*, *107*(12), 3493–3508. http://doi.org/10.1152/jn.00821.2011

Amano, K., Wandell, B. A., & Dumoulin, S. O. (2009). Visual Field Maps, Population Receptive Field Sizes, and Visual Field Coverage in the Human MT+ Complex. *Journal of Neurophysiology*, *102*(5), 2704–2718. http://doi.org/10.1152/jn.00102.2009

Auerbach, E., & Peachey, N. S. (1984). Interocular transfer and dark adaptation to long-wave test lights. *Vision Research*, *24*(9), 1043–1048.

Baker, D. H., & Meese, T. S. (2012). Interocular transfer of spatial adaptation is weak at low spatial frequencies. *Vision Res*, *63*, 81–7. http://doi.org/10.1016/j.visres.2012.05.002

Baker, D. H., Meese, T. S., & Georgeson, M. A. (2013). Paradoxical psychometric functions ("swan functions") are explained by dilution masking in four stimulus dimensions. *Iperception*, *4*(1), 17–35. http://doi.org/10.1068/i0552

Bex, P. J., Metha, A. B., & Makous, W. (1999). Enhanced motion aftereffect for complex motions. *Vision Research*, *39*(13), 2229–2238.

Bjorklund, R. A., & Magnussen, S. (1981). A study of interocular transfer of spatial adaptation. *Perception*, *10*, 511–8.

Blakemore, C., & Campbell, F. W. (1969). On the existence of neurones in the human visual system selectively sensitive to the orientation and size of retinal images. *J Physiol*, *203*, 237–60.

Blakemore, C., & Sutton, P. (1969). Size adaptation: a new aftereffect. *Science*, *166*(902), 245–7.

Blake, R., Overton, R., & Lema-Stern, S. (1981). Interocular transfer of visual aftereffects. *J Exp Psychol Hum Percept Perform*, *7*, 367–81.

Brainard, D. H. (1997). The Psychophysics Toolbox. *Spat Vis*, *10*, 433–6.

Burke, D., & Wenderoth, P. (1993). Determinants of two-dimensional motion aftereffects induced by simultaneously- and alternately-presented plaid components. *Vision Res*, *33*(3), 351–9.

Campbell, F. W., & Maffei, L. (1971). The tilt after-effect: a fresh look. *Vision Res*, *11*(8), 833–40.

Freud, S. L. (1964). The physiological locus of the spiral after-effect. *Am J Psychol*, *77*, 422–8.

Gheorghiu, E., & Kingdom, F. A. A. (2008). Spatial properties of curvature-encoding mechanisms revealed through the shape-frequency and shape-amplitude after-effects. *Vision Res*, *48*(9), 1107–24. http://doi.org/10.1016/j.visres.2008.02.002

Graziano, M. S., Andersen, R. A., & Snowden, R. J. (1994). Tuning of MST neurons to spiral motions. *The Journal of Neuroscience: The Official Journal of the Society for Neuroscience*, *14*(1), 54–67.

Holland, H. C. (1957). The Archimedes spiral. *Nature*, *179*(4556), 432–433.

Holliday, I. E., & Meese, T. S. (2008). Optic flow in human vision: MEG reveals a foveo-fugal bias in V1, specialization for spiral space in hMSTs, and global motion sensitivity in the IPS. *Journal of Vision*, *8*(10), 17.1–24. http://doi.org/10.1167/8.10.17

Kaunitz, L., Fracasso, A., & Melcher, D. (2011). Unseen complex motion is modulated by attention and generates a visible aftereffect. *Journal of Vision*, *11*(13), 10–10. http://doi.org/10.1167/11.13.10

Keck, M. J., & Price, R. L. (1982). Interocular transfer of the motion aftereffect in strabismus. *Vision Res*, *22*(1), 55–60.

Kompaniez, E., Sawides, L., Marcos, S., & Webster, M. A. (2013). Adaptation to interocular differences in blur. *J Vis*, *13*(6), art. 19. http://doi.org/10.1167/13.6.19

Kremláček, J., Kuba, M., Kubová, Z., & Chlubnová, J. (2004). Motion-onset VEPs to translating, radial, rotating and spiral stimuli. *Documenta Ophthalmologica*, *109*(2), 169–175. http://doi.org/10.1007/s10633-004-4048-7

Lee, A. L. F., & Lu, H. (2012). Two forms of aftereffects induced by transparent motion reveal multilevel adaptation. *Journal of Vision*, *12*(4), 3–3. http://doi.org/10.1167/12.4.3

Lee, A. L. F., & Lu, H. (2014). Global-motion aftereffect does not depend on awareness of the adapting motion direction. *Attention, Perception, & Psychophysics*, *76*(3), 766–779. http://doi.org/10.3758/s13414-013-0609-8

Liu, W., Zhang, Z.-J., Zhao, Y.-J., Liu, Z.-F., & Li, B.-C. (2013). Effects of Awareness on Numerosity Adaptation. *PLoS ONE*, *8*(10), e77556. http://doi.org/10.1371/journal.pone.0077556

Maruya, K., Watanabe, H., & Watanabe, M. (2008). Adaptation to invisible motion results in low-level but not high-level aftereffects. *Journal of Vision*, *8*(11), 7–7. http://doi.org/10.1167/8.11.7

Mather, G., Pavan, A., Campana, G., & Casco, C. (2008). The motion aftereffect reloaded.

Trends Cogn Sci, *12*(12), 481–7. http://doi.org/10.1016/j.tics.2008.09.002

McColl, S. L., & Mitchell, D. E. (1998). Stereodeficient subjects show substantial differences in interocular transfer of two motion adaptation aftereffects. *Vision Res*, *38*(12), 1889–900.

Meese, T. S. (1995). Using the standard staircase to measure the point of subjective equality: a guide based on computer simulations. *Percept Psychophys*, *57*(3), 267–81.

Mitchell, D. E., Reardon, J., & Muir, D. W. (1975). Interocular transfer of the motion after-effect in normal and stereoblind observers. *Exp Brain Res*, *22*(2), 163–73.

Morgan, M. (2013). Sustained attention is not necessary for velocity adaptation. *J Vis*, *13*(8), art. 26. http://doi.org/10.1167/13.8.26

Morgan, M., Dillenburger, B., Raphael, S., & Solomon, J. A. (2012). Observers can voluntarily shift their psychometric functions without losing sensitivity. *Atten Percept Psychophys*, *74*(1), 185–93. http://doi.org/10.3758/s13414-011-0222-7

Morrone, M. C., Tosetti, M., Montanaro, D., Fiorentini, A., Cioni, G., & Burr, D. C. (2000). A cortical area that responds specifically to optic flow, revealed by fMRI. *Nature Neuroscience*, *3*(12), 1322–1328. http://doi.org/10.1038/81860

Moulden, B. (1980). After-effects and the integration of patterns of neural activity within a channel. *Philos Trans R Soc Lond B Biol Sci*, *290*(1038), 39–55.

Nishida, S., & Ashida, H. (2000). A hierarchical structure of motion system revealed by interocular transfer of flicker motion aftereffects. *Vision Res*, *40*(3), 265–78.

O'Shea, R. P., & Crassini, B. (1981). Interocular transfer of the motion after-effect is not reduced by binocular rivalry. *Vision Res*, *21*(6), 801–4.

Ouhnana, M., Bell, J., Solomon, J. A., & Kingdom, F. A. A. (2013). Aftereffect of perceived regularity. *Journal of Vision*, *13*(8), art. 18. http://doi.org/10.1167/13.8.18

Pelli, D. G. (1997). The VideoToolbox software for visual psychophysics: transforming numbers into movies. *Spat Vis*, *10*, 437–42.

Raymond, J. E. (1993). Complete interocular transfer of motion adaptation effects on motion coherence thresholds. *Vision Res*, *33*(13), 1865–70.

Reuter, T. (2011). Fifty years of dark adaptation 1961-2011. *Vision Res*, *51*(21-22), 2243–62. http://doi.org/10.1016/j.visres.2011.08.021

Scarfe, P., & Johnston, A. (2011). Global motion coherence can influence the representation of ambiguous local motion. *Journal of Vision*, *11*(12), 6–6. http://doi.org/10.1167/11.12.6

Serrano-Pedraza, I., & Derrington, A. M. (2010). Antagonism between fine and coarse motion sensors depends on stimulus size and contrast. *J Vis*, *10*(8), 18. http://doi.org/10.1167/10.8.18

Smith, A. T., & Hammond, P. (1985). The pattern specificity of velocity aftereffects. *Exp Brain Res*, *60*(1), 71–8.

Smith, A. T., & Over, R. (1979). Motion aftereffect with subjective contours. *Percept Psychophys*, *25*(2), 95–8.

Snowden, R. J., & Milne, A. B. (1997). Phantom motion after effects--evidence of detectors for the analysis of optic flow. *Current Biology: CB*, *7*(10), 717–722.

Steiner, V., Blake, R., & Rose, D. (1994). Interocular transfer of expansion, rotation, and translation motion aftereffects. *Perception*, *23*(10), 1197–202.

Strobach, T., & Carbon, C.-C. (2013). Face Adaptation Effects: Reviewing the Impact of Adapting Information, Time, and Transfer. *Frontiers in Psychology*, *4*. http://doi.org/10.3389/fpsyg.2013.00318

Symons, L. A., Pearson, P. M., & Timney, B. (1996). The aftereffect to relative motion does not show interocular transfer. *Perception*, *25*(6), 651–60.

Tao, R., Lankheet, M. J. M., van de Grind, W. A., & van Wezel, R. J. A. (2003). Velocity dependence of the interocular transfer of dynamic motion aftereffects. *Perception*, *32*(7), 855–66.

Thompson, P. (1981). Velocity after-effects: The effects of adaptation to moving stimuli on the perception of subsequently seen moving stimuli. *Vision Research*, *21*(3), 337–345. http://doi.org/10.1016/0042-6989(81)90161-9

Thompson, S. P. (1880). Optical illusions of motion. *Brain*, *3*, 289–298.

Timney, B., Symons, L. A., Wilcox, L. M., & O'Shea, R. P. (1996). The effect of dark and equiluminant occlusion on the interocular transfer of visual aftereffects. *Vision Research*, *36*(5), 707–715.

Verstraten, F. A., Fredericksen, R. E., Van Wezel, R. J., Lankheet, M. J., & Van de Grind, W. A. (1996). Recovery from adaptation for dynamic and static motion aftereffects: evidence for two mechanisms. *Vision Res*, *36*(3), 421–4.

Wade, N. J. (1976). On interocular transfer of the movement aftereffect in indivuals with and without normal binocular vision. *Perception*, *5*(1), 113–8.

Webster, M. A. (2011). Adaptation and visual coding. *J Vis*, *11*(5), art. 3. http://doi.org/10.1167/11.5.3

